Comparison of Longitudinal Changes in Functional and Structural Measures for Evaluating Progression of Glaucomatous Optic Neuropathy

Kenji Suda,[1] Masanori Hangai,[1] Tadamichi Akagi,[1] Hisashi Noma,[2] Yugo Kimura,[1] Tomoko Hasegawa,[1] Hiroshi Yamada,[1] Munemitsu Yoshikawa,[1] Hideo Nakanishi,[1] Hanako Ohashi Ikeda,[1] and Nagahisa Yoshimura[1]

[1]Department of Ophthalmology and Visual Sciences, Kyoto University Graduate School of Medicine, Shogoin, Sakyo-ku, Kyoto, Japan
[2]Department of Data Science, The Institute of Statistical Mathematics, Tachikawa, Tokyo, Japan

Correspondence: Tadamichi Akagi, Department of Ophthalmology and Visual Sciences, Kyoto University Graduate School of Medicine, 54 Shougoin Kawahara-cho, Sakyo-ku, Kyoto 606-8507, Japan; akagi@kuhp.kyoto-u.ac.jp.

Submitted: February 18, 2015
Accepted: July 14, 2015

Citation: Suda K, Hangai M, Akagi T, et al. Comparison of longitudinal changes in functional and structural measures for evaluating progression of glaucomatous optic neuropathy. *Invest Ophthalmol Vis Sci*. 2015;56:5477–5484. DOI:10.1167/iovs.15-16704

Purpose. We compared longitudinal changes in functional and structural measures in eyes with glaucomatous optic neuropathy.

Methods. Circumpapillary retinal nerve fiber layer thickness (cpRNFL) and macular ganglion cell complex thickness (mGCC) were measured using spectral-domain optical coherence tomography (SD-OCT; RTVue). The Spectralis HRA+OCT instrument also was used to measure cpRNFL, and Heidelberg retina tomography II (HRT) and standard automated perimetry (SAP) were performed. Assessments were performed every 3 months over several years. Linear mixed modeling was used to evaluate the rate of change in each measure.

Results. Totals of 1406 RTVue, 1366 Spectralis, 1245 HRT, and 1392 SAP measurements were analyzed. Average baseline SAP mean deviation (MD) was −6.24 ± 5.46 dB. Linear mixed modeling revealed that SAP MD changed by −0.23 dB/y (95% confidence interval [CI], −0.34 to −0.12 dB/y). Significant negative trends also were detected in cpRNFL (RTVue, −0.41 μm/y [95% CI, −0.67 to −0.16 μm/y]; Spectralis, −1.36 μm/y [95% CI, −1.65 to −1.07 μm/y]; and mGCC (RTVue, −0.47 μm/y [95% CI, −0.64 to −0.30 μm/y]). Disc rim area remained constant over time (HRT, −0.01 mm^2/y [95% CI, −0.03 to 0.01 mm^2/y]). The SAP MD, RTVue mGCC, and Spectralis cpRNFL showed the fastest changes in the inferior retina (superior visual field), while RTVue cpRNFL changed the fastest in the superior retina.

Conclusions. Functional (SAP) and structural (SD-OCT) testing can detect longitudinal changes of glaucomatous optic neuropathy, but in different ways.

Keywords: glaucoma progression, optical coherence tomography, visual field

Accurate detection of glaucoma progression is essential for effective patient management; however, it remains a diagnostic challenge.[1,2] Although automated static perimetry is one of the most widely used methods for evaluating glaucoma progression, short- and long-term fluctuations limit the accuracy of clinician judgments.[3–5] Therefore, more objective and sensitive methods for detecting glaucoma progression are required. Detecting structural changes in the optic disc and retinal nerve fiber layer (RNFL) is one strategy for identifying glaucoma progression.[6] Although stereoscopic optic nerve head (ONH) and red-free fundus photographs can be useful in detecting detailed optic nerve and RNFL changes, respectively, interpretation of these images is largely subjective and images are susceptible to testing variability.[7]

Advances in tomographic imaging technology have made it possible to objectively evaluate structural changes in the optic disc and RNFL.[8–13] Using trend analyses, a previous report showed poor agreement between detection of progressive changes in the visual field (VF), neuroretinal rim area (with Heidelberg retinal tomography), and RNFL thickness (using time-domain optical coherence tomography [OCT]).[2]

Recent advances in spectral-domain OCT (SD-OCT) have led to more reproducible measurements of circumpapillary RNFL (cpRNFL) and macular ganglion cell complex (mGCC; three innermost retinal layers at the macula) thickness.[14–17] Greater imaging reliability and decreased measurement variability may allow for more precise detection of progressive structural changes. However, some controversy exists regarding correlations between VF testing and SD-OCT examinations. Previous studies by Na et al.[12] and Leung et al.[13] using Cirrus high definition OCT detected a higher frequency of glaucoma progression with OCT than with VF testing. Miki et al.[18] also demonstrated that Spectralis HRA+OCT RNFL thickness measurements could be used to readily detect disease progression in the eyes of patients with suspected glaucoma and developing VF defects. However, other reports using trend analyses have shown poor agreement between SD-OCT and VF measurements.[11,12]

The diagnostic accuracy of the various SD-OCT systems is thought to be similar[19]; however, it is not known whether different instruments have similar glaucoma progression detection abilities. Age-related thinning of the RNFL and mGCC are thought to have a major influence on OCT measurements.[20]

Axial length,[21] disc size,[22] and signal strength[23,24] also should be considered when examining longitudinal changes in OCT measurements.

The purpose of this study was to evaluate the rate of change in structural measurements—cpRNFL thickness from two different SD-OCT systems, mGCC from one SD-OCT system, and the rim area from confocal scanning laser ophthalmoscopy—and compare these to VF test results.

Methods

Subjects

This prospective longitudinal study adhered to the tenets of the Declaration of Helsinki, and was approved by the Institutional Review Board and Ethics Committee of the Kyoto University Graduate School of Medicine. Study subjects were enrolled prospectively at Kyoto University Hospital between April 2008 and September 2009, and informed consent was obtained from all participants.

Inclusion criteria comprised the presence of a normal angle on gonioscopy and a Snellen equivalent best-corrected visual acuity (BCVA) of at least 20/20 to ensure high imaging quality. Subjects also were required to have a typical glaucomatous VF defect (as observed on standard automated perimetry [SAP] using the Swedish interactive threshold algorithm [SITA] 24-2) with corresponding stereoscopy optic disc changes (diffuse or localized narrowing of neuroretinal rim) and/or RNFL thinning. Eyes were excluded from analyses if they had a cataract, vitreoretinal disease (including patchy chorioretinal atrophy, lacquer crack lesion, and choroidal neovascularization), uveitis, pathologic myopia, prior ocular surgery, or prior laser therapy. The use of topical IOP lowering agents was permitted. Subjects also were excluded from the study if they had a neurological disease, diabetes mellitus, or any other systemic disease that might affect the eye or VF (e.g., cerebrovascular event, uncontrolled hypertension, and blood disorders). Data from subjects who developed an epiretinal membrane on the macula during follow-up were excluded because of the potential influence of these membranes on retinal thickness. To avoid introducing a selection bias, data from subjects who underwent ocular surgery during the follow-up period were included until the date of surgery.

Clinical Examinations

All subjects underwent a comprehensive ophthalmic examination at baseline involving the measurement of IOP with a Goldman applanation tonometer, and uncorrected and best-corrected visual acuity with a Landolt chart at 5 m. Subjects also underwent slit-lamp examination, gonioscopy, stereoscopic optic disc photography (3-Dx simultaneous stereo disc camera; Nidek, Gamagori, Japan), red-free fundus photography (Heidelberg Retina Angiogram 2 [HRA2]; Heidelberg Engineering, Heidelberg, Germany), SAP, Humphrey Visual Field Analyzer using the 24-2 SITA testing protocol (HFA + 24-2 SITA; Carl Zeiss-Meditec, Dublin, CA), confocal scanning laser ophthalmoscopy (Heidelberg retina tomograph [HRT] II; Heidelberg Engineering), and OCT examinations (RTVue-100; Optovue, Fremont, CA, USA and Spectralis HRA+OCT system; Heidelberg Engineering). The VF, HRT II, and OCT examinations were performed on the same day every 3 months until October 2012. Only subjects with a minimum of four study visits during the follow-up period were included. All VF and HRT II testing was performed before OCT examination.

Table 1. Subject Characteristics

n, Eyes/Patients	125/87
Age, y	47.14 ± 11.37 (21 to 71)
Sex, male/female	53/34
Spherical equivalent, diopters	−5.87 ± 3.73 (−17.00 to +2.25)
Axial length, mm	26.05 ± 1.67 (21.96 to 30.30)
MD value at entry, dB	−6.24 ± 5.46 (−27.11 to 1.63)
Follow-up period, y	2.85 ± 0.75 (0.75 to 4.00)
Glaucoma stage,* eyes	
Early, MD > −6 dB	78
Moderate, −12 dB < MD < −6 dB	29
Advanced, MD < −12dB	18

Data presented as mean ± SD (range).
* Classified according to VF findings.

VF Examinations

Only reliable VF tests were included in analyses. These comprised fixation loss rate, false-positive rate, and false-negative rate < 20%. A glaucomatous VF defect was defined as glaucoma hemifield test results outside normal limits, more than three significant ($P < 0.05$) and one highly significant ($P < 0.01$) nonedge contiguous points on the same side of the horizontal meridian as in the pattern deviation plot, or pattern standard deviation < 5% in an otherwise normal VF. All VF findings were confirmed in at least two consecutive testing sessions. To account for subject learning, the first VF test was not included in analyses if it was the first VF test a subject had taken.

Confocal Scanning Laser Ophthalmoscope Imaging

The HRT II was used to measure optic disc topographic features, including cup-to-disc area ratio (C/D), rim area, rim volume, and disc size. All HRT images were obtained by an experienced examiner through undilated pupils. All images were three-dimensional topographic images with a digital resolution between 384 × 384 × 16 and 384 × 384 × 64 pixels and were constructed from multiple axial focal planes along the ONH. An average of three consecutive scans was obtained and aligned to create a single topographic image. Poor quality images, defined as having a large standard deviation, were not excluded from analyses. Instead, the imaging data were adjusted using linear mixed modeling of explanatory variables (see below). As previously described,[2,25] the optic disc margin was determined using built-in HRT II software, while the examiner confirmed the disc margin viewing stereo disc images. After determining the optic disc margin, the HRT image analysis algorithm automatically placed a standard reference plane 50 μm below the retinal surface between 350° and 356°. This reference plane then was used as the zero for the topographic height of each (x, y) location included within the contour line. The relative height of each point above and below the reference plane then was arbitrarily categorized as either belonging to the neuroretinal rim or to the cup. The resultant volumes then were used to calculate C/D, rim area, and rim volume. Magnification errors were automatically corrected for by the HRT II software based upon each subject's refractive error and corneal curvature measurements.

SD-OCT Imaging

All SD-OCT images were obtained by an experienced examiner after pupillary dilation with 0.5% tropicamide and 0.5% phenylephrine.

Investigative Ophthalmology & Visual Science

TABLE 2. Linear Mixed Model Results for VF Indices, OCT cpRNFL and GCC Thickness Measurements, and Heidelberg Retinal Tomography Neuroretinal Rim Measurements

	Mean Deviation, dB	VFI, %	HRT II Neuroretinal Rim Area, mm²	RTVue GCC Thickness, μm	RTVue cpRNFL Thickness, μm	Spectralis cpRNFL Thickness, μm
n, tests	1392	1383	1245	1406	1404	1366
Tests/eye	11.14 ± 3.09	11.06 ± 3.05	9.96 ± 2.97	11.25 ± 3.12	11.23 ± 3.12	10.93 ± 3.04
Baseline β_0 (95% CI)	−6.30 (−7.34 to −5.26)	83.65 (80.57 to 86.73)	1.23 (1.14 to 1.32)	74.15 (72.30 to 75.99)	80.34 (78.52 to 82.16)	71.02 (68.66 to 73.38)
β_1' - Time, y (95% CI)	−0.23 (−0.34 to −0.12)	−0.79 (−1.08 to −0.50)	−0.010 (−0.03 to 0.01)	−0.47 (−0.64 to −0.30)	−0.41 (−0.67 to −0.16)	−1.36 (−1.65 to −1.07)
β_2' - Age, y (95% CI)	−0.14 (−0.24 to −0.04)	−0.42 (−0.73 to −0.11)	−0.005 (−0.01 to 0.00)	0.03 (0.16 to 0.21)	0.03 (−0.15 to 0.22)	−0.02 (−0.26 to 0.21)
β_3' - Axial length, mm (95% CI)	−0.96 (−1.62 to −0.29)	−2.15 (−4.14 to −0.15)	0.05 (−0.00 to 0.10)	−0.72 (−1.93 to 0.49)	−0.47 (−1.69 to 0.75)	−1.24 (−2.76 to 0.27)
β_4' - Disc size, mm²	0.16 (−1.37 to 1.69)	0.48 (−4.09 to 5.04)	0.26 (0.15 to 0.37)	0.89 (−1.86 to 3.64)	1.85 (−0.94 to 4.64)	2.81 (−0.63 to 6.26)
β_5' - Image quality (95% CI)			0.00 (−0.00 to 0.00)	−0.03 (−0.05 to −0.02)	0.06 (0.03 to 0.08)	−0.098 (−0.15 to −0.04)

The RTVue-100 was used to evaluate cpRNFL and macular GCC thickness using built-in RTVue-100 software (version 4.0). The RTVue-100 acquires 26,000 axial scans (A-scans) per second and has a 5-μm depth resolution in tissue. To measure cpRNFL thickness, the "RNFL 3.45" scan mode was used. This scanning protocol acquires four 3.45-mm diameter circular scans centered on the optic disc. The final scan is the average of 1024 individual A-scans. Macular GCC thickness was measured using the "GCC" scan mode, which acquires 14,928 A-scans over a 7×7 mm² area. The scan is acquired in 0.58 seconds and is comprised of 15 vertical scans spaced 0.5 mm apart. The center of the GCC scan was shifted 1.0 mm in the temporal direction to improve temporal periphery imaging. After GCC scans were acquired, the RTVue-100 software automatically calculated average GCC thickness within a 6-mm diameter circular area centered on the fovea.

The Spectralis HRA+OCT system also was used to evaluate cpRNFL thickness. The eye tracking system of this instrument allows accurate averaging of up to 100 B-scans (7-μm axial resolution) acquired at an identical location. This averaging efficiently reduces speckle noise. For cpRNFL imaging, we performed a 3.46-mm diameter circular scan, consisting of 1536 A-scans, centered on the optic disc. A total of 16 scans was acquired and averaged to obtain the final scan for analysis.

Statistical Analyses

Longitudinal time trends of outcome measurements were evaluated using linear mixed models fitted with random intercepts and coefficients at the subject and eye level. Linear mixed-effects modeling allowed the determination of correlations among repeated measurements and for instances when both eyes of a single subject were included.[26] Linear mixed-effects models also can manage data-sets with multiple missing data points or with high variation in examination times.

Equation 1 describes the corrections applied to the data

$$Y_{ijt} = \beta_0 + \beta_1 \text{TIME} + \zeta_{0j} + \zeta_{1j} \times \text{TIME} + \zeta_{0i|j} + \zeta_{1i|j} \times \text{TIME} + \varepsilon_{ijt}, \quad (1)$$

where Y_{ijt} = individual measurements at visit t; β_0, β_1 = fixed-effects coefficients; ζ_{0j}, ζ_{1j} = random patient effects associated with the intercept and time slope; and $\zeta_{0i|j}$, $\zeta_{1i|j}$ = random effects associated with the inclusion of both eyes of a single subject.

To account for the influence of age, axial length, disc size, and image quality, results also were analyzed using a linear mixed model adjusted for age, axial length, disc size, and image quality as fixed effects. To adjust for differences in imaging quality, tomography standard deviation, signal strength index (SSI), and quality (Q) were used to adjust HRTII, RTVue, and Spectralis data, respectively. Equation 2 describes the adjusting formula for linear mixed modeling, as follows:

$$\begin{aligned} Y_{ijt} = {} & \beta_0' + \beta_1' \text{TIME} + \beta_2' \text{Age} + \beta_3' \text{Axial length} \\ & + \beta_4' \text{Disc size} + \beta_5' \text{Imaging Quality}^* \\ & + \zeta_{0j} + \zeta_{1j} \times \text{TIME} + \zeta_{0i|j} + \zeta_{1i|j} \times \text{TIME} + \varepsilon_{ijt}, \end{aligned} \quad (2)$$

where * indicates for morphological testing only.

Baseline measurements were evaluated using the intercepts determined from linear mixed models without adjustment for age, axial length, disc size, or imaging quality. Time trends were evaluated as the average rate of change per year and were calculated using the linear mixed model after adjusting for age, axial length, disc size, and image quality.

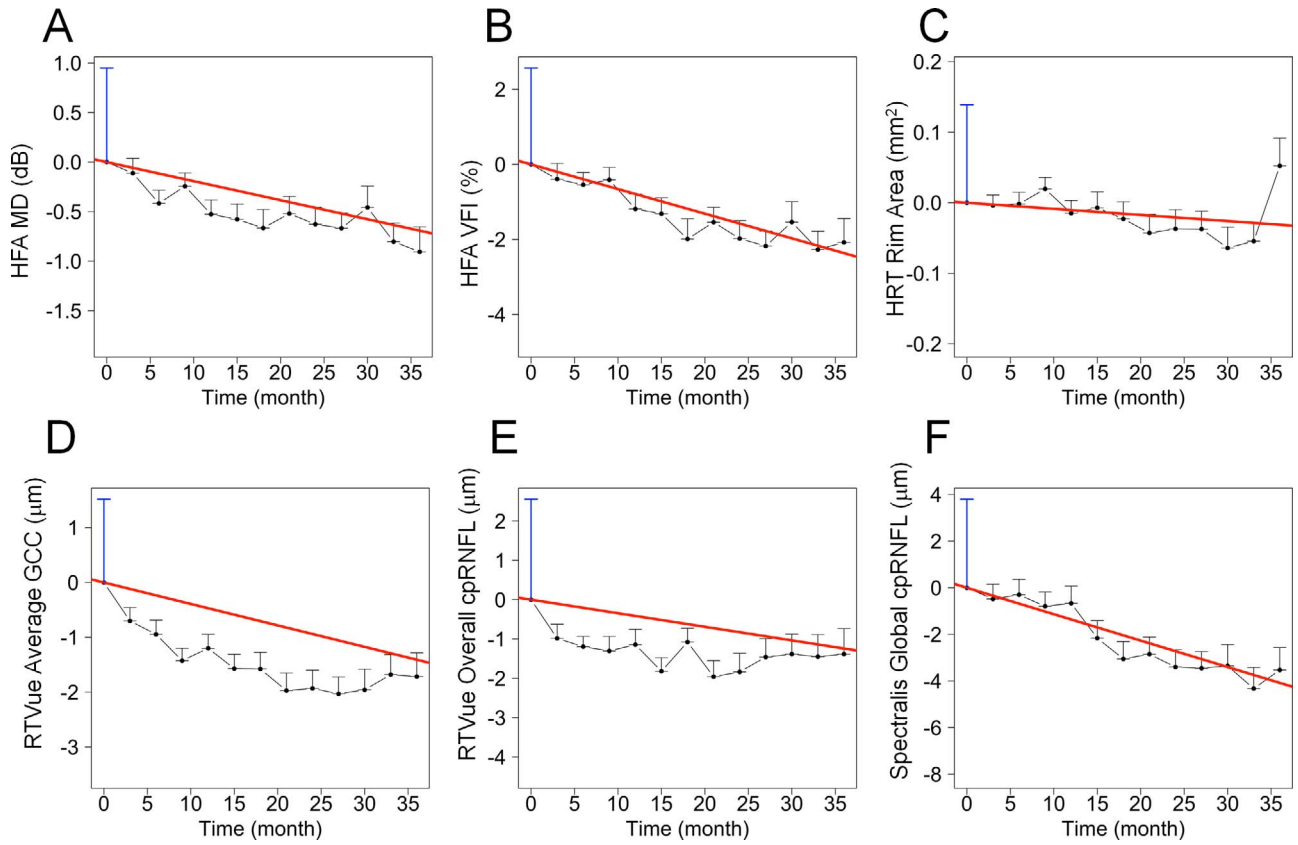

Figure 1. Regression lines calculated from the linear mixed model of Humphrey field analyzer mean deviation (HFA MD, [**A**]), VF index (VFI, [**B**]), Heidelberg retinal tomograph II (HRT II) rim area (**C**), RTVue mGCC (**D**), RTVue cpRNFL (**E**), and Spectralis RTVue cpRNFL (**F**). Each data point indicates the average change from baseline for all patients examined at a given time point. The *black error bar* represents standard error, the *red line* represents the regression line calculated with the linear mixed model, and the *blue error bar* at baseline represents the residual from the linear mixed model.

To compare test–retest variability, we examined the residuals obtained from the linear mixed model and the standard deviation of regression line residuals in each eye, as previously described.[27] To evaluate the test–retest variability in the growth curve model, the rate of change with time should be considered. Using linear mixed modeling, we excluded the influence of the rate of change with time from the residual. We assessed the within-subject variance of each examination with the residual gained from the linear mixed model (after adjustment for age, axial length, disc size, and imaging quality) and the mean standard deviation of the residuals from the regression line. To evaluate the individual heterogeneity of time trends in each eye examined, estimates of best linear unbiased predictors (BLUPs) also were calculated and analyzed in this linear mixed model after adjustment.[28]

All P values presented are 2-sided values. Statistical significance was defined as $P < 0.05$. All analyses were performed using SPSS (ver. 20.0; IBM Corporation, Armonk, NY, USA) and R (ver. 3.0.1; R Foundation for Statistical Computing, Vienna, Austria) statistical software.

Results

A total of 138 eyes of 94 subjects was prospectively enrolled, and 13 eyes of seven subjects were retrospectively excluded because an epiretinal membrane or chorioretinal atrophy was detected on color photographs during follow-up. Therefore, 125 eyes of 87 patients were included in this study. Subject baseline characteristics are shown in Table 1. The mean follow-up period was 2.85 ± 0.75 years. For 43 patients, the baseline VF test was the first VF test the subject had ever taken. Therefore, results from the first VF testing session at baseline for these subjects were excluded from analyses.

Totals of 1392 VF data points, 1245 HRT II data points, 1406 RTVue data points, and 1366 Spectralis OCT data points were collected for an average of 11.14, 9.96, 11.25, and 10.93 observations per eye, respectively (Table 2). At baseline, 18 eyes (14.4%) had advanced glaucoma (VF mean deviation [MD] < -12 dB), 29 eyes (23.2%) had moderate glaucoma (-12 dB $\leq$ MD ≤ -6 dB), and 78 eyes (62.4%) had early glaucoma (MD > -6 dB).

Changes in Measurements Over Time

Linear mixed models for evaluating longitudinal trend analyses are presented in Table 2, Supplementary Table S1, and Figure 1. Linear mixed modeling showed an estimated average VF MD rate of change of -0.23 dB/y ($P < 0.001$). Significant negative trends over time also were detected for average cpRNFL and macular GCC parameters (both $P < 0.001$). Trends over time for HRT rim area were not significantly different from zero ($P = 0.38$, Table 2).

Influence of Age, Axial Length, Disc Size, and Image Quality

Linear mixed modeling with adjustments revealed the influence of age, axial length, disc size, and image quality for each

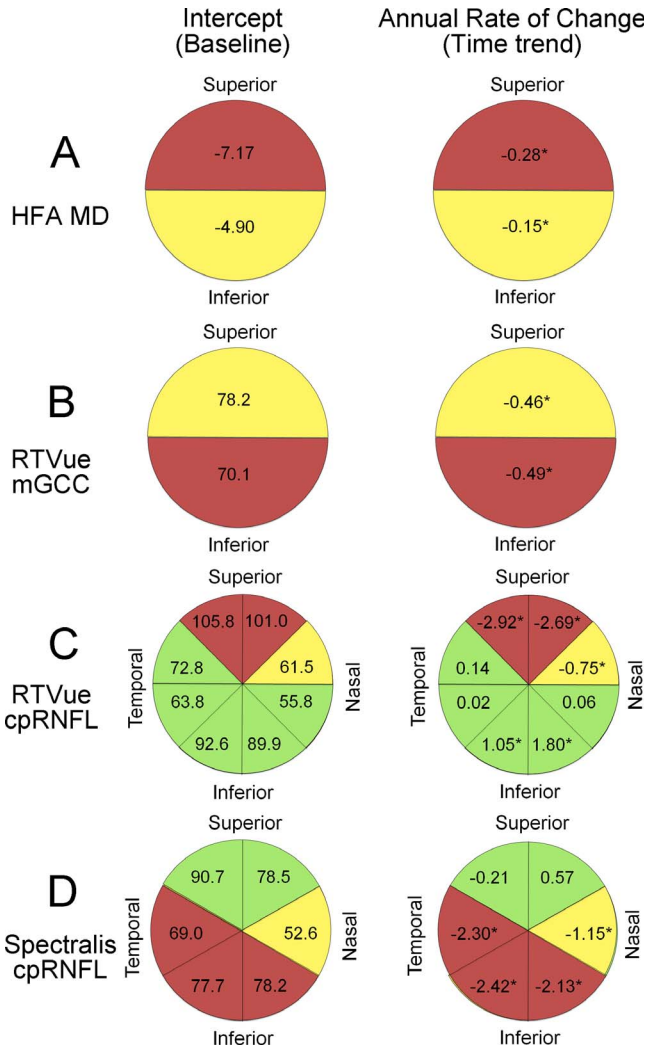

FIGURE 2. Baseline values and changes over time in sectorial indices, as calculated from linear mixed models for HFA MD (**A**), RTVue mGCC (**B**), RTVue cpRNFL (**C**), and Spectralis RTVue cpRNFL (**D**). *$P < 0.01$.

parameter measured (Table 2). Significant negative correlations were found between age and VF parameters, but not for HRT II and SD-OCT measurements. A significant negative correlation also was found between axial length and VF MD, but not between axial length and HRT II rim area or between axial length and any of the three SD-OCT measurements. With the exception of HRT II rim area (positive correlation), disc size did not significantly correlate with any of the other measurements. Significant negative correlations were found between image quality and RTVue GCC thickness and Spectralis cpRNFL thickness. Significant positive correlations were found between image quality and RTVue cpRNFL thickness; however, HRT II rim area was not significantly influenced by image quality.

Changes in Retinal and ONH Sectors Over Time

Analyses of retinal and ONH sectors with linear mixed models for evaluating longitudinal trends are presented in Supplementary Table S1 and Figure 2. As shown in Figure 2, VF MD, RTVue GCC thickness, and Spectralis cpRNFL thickness had greater negative rates of change in inferior morphological sectors (superior VF sector). However, RTVue cpRNFL thickness had the largest negative rate of change in the superior quadrant.

Test–Retest Variability for Each Measured Parameter

Test–retest variability in longitudinal data was evaluated using residuals obtained from linear mixed modeling. This was performed to determine likely causes of differences in detectability of time trends and sectorial index differences. As shown in Figure 1 and Supplementary Table S1, the ratios of HRT II rim area and RTVue cpRNFL thickness residuals to their annual rate of change were greater than for the other three average indices (i.e., VF MD, RTVue GCC thickness, and Spectralis cpRNFL thickness). Figure 3 presents histograms of the residual standard deviations from the regression line estimated with linear mixed modeling. These results also indicated that the mean of residual standard deviations for HRT II and RTVue cpRNFL thickness were much greater than the annual rate of change calculated with linear mixed modeling. However, this was not the case for the other three average indices.

Correlations Between Parameter Changes Over Time in Individual Eyes

Supplementary Figure S1 shows the correlations between parameter changes over time. Parameter trends over time were compared using BLUP estimates from linear mixed modeling. Changes in VF parameters were poorly correlated with imaging parameters (correlation coefficients = 0.08–0.23), despite VF indices changes (MD and VFI) exhibiting a strong correlation with each other (correlation coefficient = 0.87). However, the correlation between imaging tests also was poor, even between different OCT systems (correlation coefficients = 0.047–0.30).

DISCUSSION

To the best of our knowledge, this is the first study to compare the different glaucoma progression evaluation SD-OCT devices (i.e., RTVue and Spectralis). Because RTVue is the first SD-OCT system that allows measurement and analysis of cpRNFL and GCC thickness,[14–16] the present findings may aid the interpretation of RTVue data in clinical practice. Ultra-high resolution Spectralis images, achieved through a combination of confocal laser scanning ophthalmoscopy and real-time 3-dimensional eye tracking, are expected to allow more precise detection of glaucoma progression compared to other SD-OCT images.[29] In this study, we directly compared the ability of different SD-OCT systems to evaluate glaucoma progression. Leung et al.[30] previously showed that Cirrus HD-OCT outperformed Stratus OCT because it detected a larger number of eyes with RNFL progression. However, the Stratus OCT is a time-domain system and cannot accurately evaluate the thickness of a particular retinal layer. Another Cirrus HD-OCT study demonstrated that macular ganglion cell and inner plexiform layer changes were more sensitive indicators of glaucoma progression than cpRNFL thickness changes.[11]

Our findings revealed that significant changes were longitudinally detectable with VF testing and both types of SD-OCT, but not with HRT II. In addition, analyses of sectorial indices suggest that only RTVue cpRNFL thickness shows different results from VF testing and other OCT measurements. According to Hood et al.,[31] the inferior macular region is more vulnerable to glaucomatous changes. Our results supported this argument, showing that changes in SAP MD values are

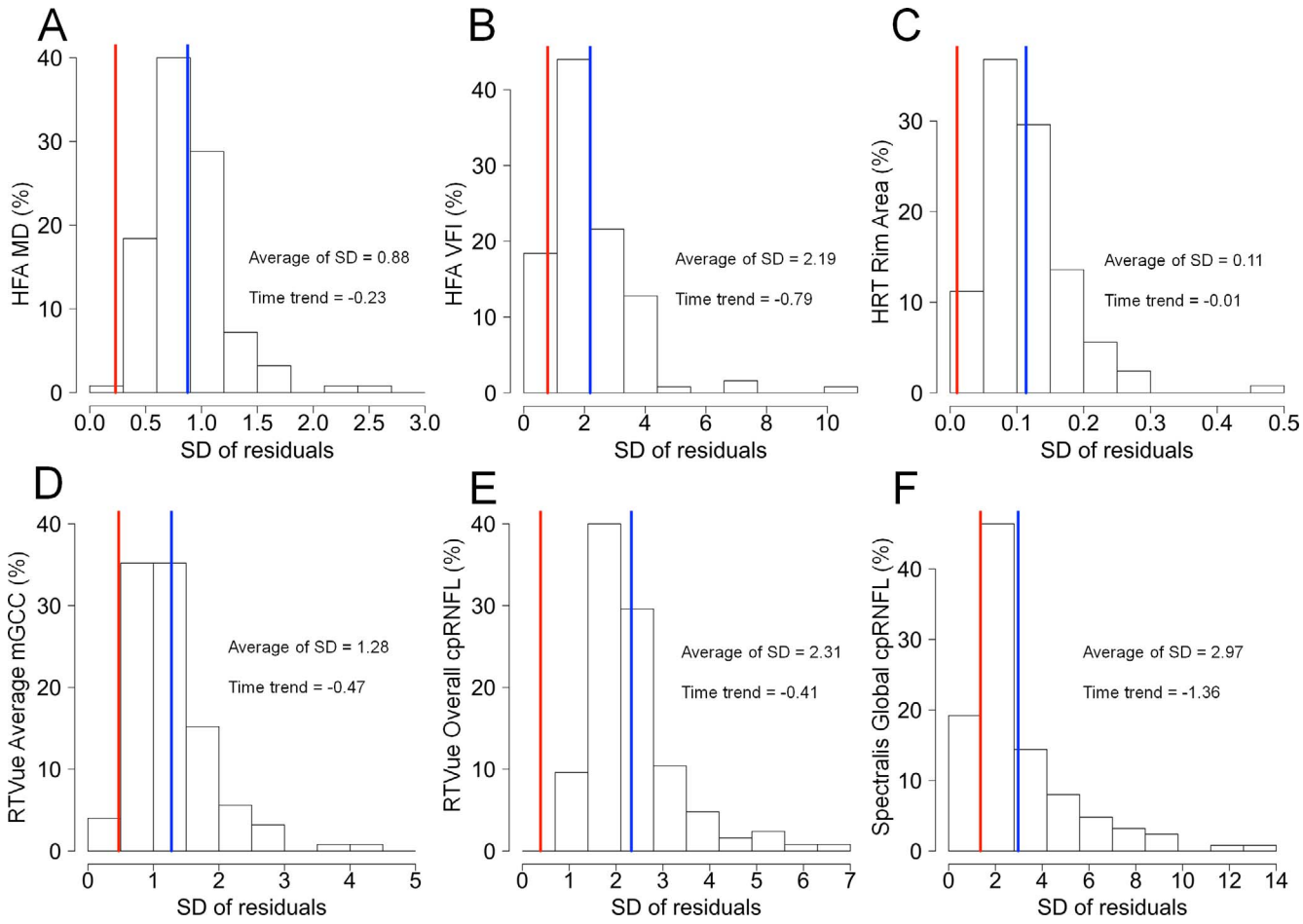

Figure 3. Histograms of the standard deviations of residuals from the regression line, as estimated with linear mixed models for HFA MD (**A**), VFI (**B**), HRT II rim area (**C**), RTVue mGCC (**D**), RTVue cpRNFL (**E**), and Spectralis RTVue cpRNFL (**F**). The *blue vertical bar* represents the average standard deviation of residuals. The *red vertical bar* represents the annual change (time trend) that was calculated from the linear mixed model.

more severe in the upper VF hemifield. Together, these findings suggested that our RTVue cpRNFL measurements may have produced more variable sectorial analysis findings.

To improve our understanding of the origin of this variability, we examined the residuals obtained from linear mixed modeling. This was performed because residuals from linear mixed modeling represent test–retest variability. Chauhan et al.[3] previously showed that test–retest variability inhibits the ability to detect glaucoma progression, even in eyes with rapid progression. Comparisons between parameter rates of change and the residuals revealed that HRT II and RTVue cpRNFL thickness have greater residuals compared to the rate of change of VF MD, RTVue GCC thickness, and Spectralis cpRNFL thickness. This may explain why the HRT II indices had a lower ability to detect glaucoma progression and why sectorial analyses of RTVue cpRNFL thickness produced varying results.

However, our results were inconsistent with those obtained by Leung et al.,[2] which showed that HRT and cpRNFL thickness could be used to detect glaucoma progression. One of the reasons why the longitudinal change with HRT II was not significant in our study may relate to the manner in which topographic parameters were measured with this device. Once the disc margin is defined, the reference plane is set 50 μm below the surface. As the volume of rim decreases over time, the reference plane moves down simultaneously. Therefore, the rim area (for instance) is unlikely to change over time. This phenomenon would be applicable to the previous study that demonstrated the poor performance of HRT in detecting longitudinal changes.[32]

Another reason may be the poor segmentation accuracy or misplacement of the measurement location. In particular, due to the fact that numerous high myopes were included in our study, there may have been issues involving the HRT II algorithm determining the standard reference plane required for ONH rim and cup demarcation. When we measured cpRNFL thickness using SD-OCT, the manual placement of the measurement location may have differed between visits in each subject. Improved fundus visualization with the Spectralis infrared images may inherently increase the reproducibility of the measurement location. Unlike RTVue cpRNFL thickness, RTVue GCC thickness had a relatively low test–retest variability. This is likely due to the fact that GCC thickness was obtained from scans created by averaging 15 individual vertical scans and because the easily determined foveal center was used as a reference point.

Axial length significantly affected our GCC measurements, as indicated by linear mixed modeling results after adjustment. Lim et al.[33] reported that the parafoveal retina became thinner and the fovea became thicker as axial length increased in healthy eyes. However, this finding is not completely applicable to our results because full macular thickness was measured and a time-domain OCT system was used. However, care still should be taken to account for the effect of axial

length on GCC thickness in eyes with glaucoma. Shoji et al.[34] reported that GCC thickness is the most suitable measure for diagnosing glaucoma in myopic eyes. We reported a significant change in GCC thickness over time. Therefore, we support the argument that GCC thickness is useful for the evaluation of glaucoma progression, despite being influenced by axial length. Consistent with a previous study,[21] we found little impact of axial length on cpRNFL thickness.

Our findings also revealed that signal strength was significantly correlated with all three SD-OCT measurement indices. Other studies have suggested that image signal strength can influence OCT retinal thickness measurements[21,23,24] and that this effect varies for different SD-OCT systems and retinal thickness indices.[24,35] In our study, the extent and direction of influence by image quality varied, indicating that the respective influence of image quality should be considered for each device.

This study has some limitations. First, our study population was relatively small and biased toward an early glaucoma stage and myopia, because elderly subjects often exhibit other ocular diseases, such as cataract. Therefore, care should be taken when applying our results to other subject groups. More optimized devices for myopia (e.g., with a refraction-adjusting tool[36] or measurements of cpRNFL with a larger diameter) may improve the accuracy of evaluations; this should be investigated in future studies. Second, this study was designed around a linear progression of glaucoma. However, several studies have suggested that glaucoma progression is nonlinear.[31,37,38] Nonlinear glaucoma progression could explain why the intrasubject VF and morphology measurement correlation was poor. This is because the BLUP methods used in these analyses are based on a linear progression.[31,38] Further research with nonlinear models is required to improve our understanding of the relationship between retinal and optic nerve function and structure in glaucomatous eyes. Third, we adopted linear mixed model for the evaluation of each device; however, it should be noted that the statistical significance of time trend in the analyses by linear mixed models does not necessarily imply "detection of progression." The *P* values from the linear mixed models simply inform us if the rate of decay of the sample was significantly negative, taking into account the distribution of random intercepts and random slopes of correlated errors. Additionally, the significance of the variables coefficient would depend on specific parameters, such as within- and between-subject variability. Therefore, these results do not necessarily indicate if individual subjects progressed (yes versus no) and should, therefore, be interpreted carefully.

In conclusion, VF testing and morphological examinations detected significant longitudinal changes in the study population; however, the capability for detection varied between methods, even between structural evaluation methods.

Acknowledgments

Supported in part by a Grant-in-Aid for Scientific Research (25462713) from the Japan Society for the Promotion of Science (JSPS). The authors alone are responsible for the content and writing of this paper.

Disclosure: **K. Suda**, None; **M. Hangai**, None; **T. Akagi**, None; **H. Noma**, None; **Y. Kimura**, None; **T. Hasegawa**, None; **H. Yamada**, None; **M. Yoshikawa**, None; **H. Nakanishi**, None; **H.O. Ikeda**, None; **N. Yoshimura**, None

References

1. Medeiros FA, Zangwill LM, Alencar LM, et al. Detection of glaucoma progression with stratus OCT retinal nerve fiber layer, optic nerve head, and macular thickness measurements. *Invest Ophthalmol Vis Sci*. 2009;50:5741–5748.
2. Leung CK, Liu S, Weinreb RN, et al. Evaluation of retinal nerve fiber layer progression in glaucoma: a prospective analysis with neuroretinal rim and visual field progression. *Ophthalmology*. 2011;118:1551–1557.
3. Chauhan BC, Garway-Heath DF, Goni FJ, et al. Practical recommendations for measuring rates of visual field change in glaucoma. *Br J Ophthalmol*. 2008;92:569–573.
4. Artes PH, Chauhan BC. Longitudinal changes in the visual field and optic disc in glaucoma. *Prog Retin Eye Res*. 2005;24:333–354.
5. Flammer J, Drance SM, Zulauf M. Differential light threshold. Short- and long-term fluctuation in patients with glaucoma, normal controls, and patients with suspected glaucoma. *Arch Ophthalmol*. 1984;102:704–706.
6. Quigley HA, Katz J, Derick RJ, et al. An evaluation of optic disc and nerve fiber layer examinations in monitoring progression of early glaucoma damage. *Ophthalmology*. 1992;99:19–28.
7. Jampel HD, Vitale S, Ding Y, et al. Test-retest variability in structural and functional parameters of glaucoma damage in the glaucoma imaging longitudinal study. *J Glaucoma*. 2006;15:152–157.
8. Wollstein G, Garway-Heath DF, Fontana L, Hitchings RA. Identifying early glaucomatous changes. Comparison between expert clinical assessment of optic disc photographs and confocal scanning ophthalmoscopy. *Ophthalmology*. 2000;107:2272–2277.
9. Medeiros FA, Zangwill LM, Bowd C, et al. Use of progressive glaucomatous optic disk change as the reference standard for evaluation of diagnostic tests in glaucoma. *Am J Ophthalmol*. 2005;139:1010–1018.
10. Alencar LM, Zangwill LM, Weinreb RN, et al. Agreement for detecting glaucoma progression with the GDx guided progression analysis, automated perimetry, and optic disc photography. *Ophthalmology*. 2010;117:462–470.
11. Na JH, Sung KR, Baek S, et al. Detection of glaucoma progression by assessment of segmented macular thickness data obtained using spectral domain optical coherence tomography. *Invest Ophthalmol Vis Sci*. 2012;53:3817–3826.
12. Na JH, Sung KR, Lee JR, et al. Detection of glaucomatous progression by spectral-domain optical coherence tomography. *Ophthalmology*. 2013;120:1388–1395.
13. Leung CK, Yu M, Weinreb RN, et al. Retinal nerve fiber layer imaging with spectral-domain optical coherence tomography: patterns of retinal nerve fiber layer progression. *Ophthalmology*. 2012;119:1858–1866.
14. Guedes V, Schuman JS, Hertzmark E, et al. Optical coherence tomography measurement of macular and nerve fiber layer thickness in normal and glaucomatous human eyes. *Ophthalmology*. 2003;110:177–189.
15. Tan O, Chopra V, Lu AT, et al. Detection of macular ganglion cell loss in glaucoma by Fourier-domain optical coherence tomography. *Ophthalmology*. 2009;116:2305–2314.e2.
16. Seong M, Sung KR, Choi EH, et al. Macular and peripapillary retinal nerve fiber layer measurements by spectral domain optical coherence tomography in normal-tension glaucoma. *Invest Ophthalmol Vis Sci*. 2010;51:1446–1452.
17. Mori S, Hangai M, Sakamoto A, Yoshimura N. Spectral-domain optical coherence tomography measurement of macular volume for diagnosing glaucoma. *J Glaucoma*. 2010;19:528–534.
18. Miki A, Medeiros FA, Weinreb RN, et al. Rates of retinal nerve fiber layer thinning in glaucoma suspect eyes. *Ophthalmology*. 2014;121:1350–1358.
19. Leite MT, Rao HL, Zangwill LM, et al. Comparison of the diagnostic accuracies of the Spectralis, Cirrus, and RTVue

optical coherence tomography devices in glaucoma. *Ophthalmology*. 2011;118:1334–1339.

20. Leung CK, Ye C, Weinreb RN, et al. Impact of age-related change of retinal nerve fiber layer and macular thicknesses on evaluation of glaucoma progression. *Ophthalmology*. 2013; 120:2485–2492.
21. Hoh ST, Lim MC, Seah SK, et al. Peripapillary retinal nerve fiber layer thickness variations with myopia. *Ophthalmology*. 2006; 113:773–777.
22. Hayamizu F, Yamazaki Y, Nakagami T, Mizuki K. Optic disc size and progression of visual field damage in patients with normal-tension glaucoma. *Clin Ophthalmol*. 2013;7:807–813.
23. Cheung CY, Leung CK, Lin D, et al. Relationship between retinal nerve fiber layer measurement and signal strength in optical coherence tomography. *Ophthalmology*. 2008;115: 1347–1351, 1351.e1–1351.e2.
24. Huang J, Liu X, Wu Z, Sadda S. Image quality affects macular and retinal nerve fiber layer thickness measurements on fourier-domain optical coherence tomography. *Ophthalmic Surg Lasers Imaging*. 2011;42:216–221.
25. Kimura Y, Hangai M, Morooka S, et al. Retinal nerve fiber layer defects in highly myopic eyes with early glaucoma. *Invest Ophthalmol Vis Sci*. 2012;53:6472–6478.
26. Fitzmaurice GM, Laird NM, Ware JH. *Applied Longitudinal Analysis*. 2nd ed. Hoboken: Wiley; 2011:xxv, 701.
27. Gardiner SK, Fortune B, Demirel S. Signal-to-noise ratios for structural and functional tests in glaucoma. *Transl Vis Sci Technol*. 2013;2(6):3.
28. Medeiros FA, Zangwill LM, Weinreb RN. Improved prediction of rates of visual field loss in glaucoma using empirical Bayes estimates of slopes of change. *J Glaucoma*. 2012;21:147–154.
29. Pierro L, Gagliardi M, Iuliano L, et al. Retinal nerve fiber layer thickness reproducibility using seven different OCT instruments. *Invest Ophthalmol Vis Sci*. 2012;53:5912–5920.
30. Leung CK, Chiu V, Weinreb RN, et al. Evaluation of retinal nerve fiber layer progression in glaucoma: a comparison between spectral-domain and time-domain optical coherence tomography. *Ophthalmology*. 2011;118:1558–1562.
31. Hood DC, Kardon RH. A framework for comparing structural and functional measures of glaucomatous damage. *Prog Retin Eye Res*. 2007;26:688–710.
32. Yoon JY, Na JK, Park CK. Detecting the progression of normal tension glaucoma: a comparison of perimetry, optic coherence tomography, and Heidelberg retinal tomography. *Korean J Ophthalmol*. 2015;29:31–39.
33. Lim MC, Hoh ST, Foster PJ, et al. Use of optical coherence tomography to assess variations in macular retinal thickness in myopia. *Invest Ophthalmol Vis Sci*. 2005;46:974–978.
34. Shoji T, Sato H, Ishida M, et al. Assessment of glaucomatous changes in subjects with high myopia using spectral domain optical coherence tomography. *Invest Ophthalmol Vis Sci*. 2011;52:1098–1102.
35. Samarawickrama C, Pai A, Huynh SC, et al. Influence of OCT signal strength on macular, optic nerve head, and retinal nerve fiber layer parameters. *Invest Ophthalmol Vis Sci*. 2010;51: 4471–4475.
36. Nakanishi H, Akagi T, Hangai M et al. Sensitivity and specificity for detecting early glaucoma in eyes with high myopia from normative database of macular ganglion cell complex thickness obtained from normal non-myopic or highly myopic Asian eyes. *Graefes Arch Clin Exp Ophthalmol*. 2015;253: 1143–1152.
37. Yu M, Weinreb RN, Yiu C, et al. Computer simulation of progressive retinal nerve fiber layer loss in glaucoma: performance of event and trend analyses. *Invest Ophthalmol Vis Sci*. 2011;52:9674–9683.
38. Harwerth RS, Wheat JL, Fredette MJ, Anderson DR. Linking structure and function in glaucoma. *Prog Retin Eye Res*. 2010; 29:249–271.

Investigative Ophthalmology & Visual Science